

**Supplementary Information For**

**“A Comparison of the Structural Collapse of Zeolitic Imidazolate Frameworks (ZIFs) and Aluminosilicate Zeolites by Ball-milling”**

*Emma F. Baxter<sup>1</sup>, Thomas D. Bennett<sup>1</sup>, Andrew Cairns<sup>2</sup>, Nick J. Brownbill<sup>3</sup>, Andrew L. Goodwin<sup>2</sup>, David A. Keen<sup>4</sup>, Philip Chater<sup>5</sup>, Frédéric Blanc<sup>3</sup> and Anthony K. Cheetham<sup>1</sup>*

*<sup>1</sup> Department of Materials Science and Metallurgy, University of Cambridge, 27 Charles Babbage Road, Cambridge, CB3 0FS, United Kingdom*

*<sup>2</sup> Inorganic Chemistry Laboratory, Department of Chemistry, University of Oxford, South Parks Road, Oxford OX1 3QR, United Kingdom*

*<sup>3</sup> Department of Chemistry and Stephenson Institute for Renewable Energy, University of Liverpool, Crown Street, Liverpool, L69 7ZD, United Kingdom*

*<sup>4</sup> ISIS Facility, Rutherford Appleton Laboratory, Harwell Oxford, Didcot, OX11 0QX, United Kingdom*

*<sup>5</sup> Diamond Light Source, Chilton, Oxfordshire OX11 0DE, United Kingdom*

## **Contents:**

### **Powder X-ray Diffraction Data**

FIGURE S1. PXRD of crystalline ZIF-4 ball milled at various times.....	S4
FIGURE S2. PXRD of crystalline ZIF-zni ball milled at various times.....	S5
FIGURE S3. PXRD of crystalline ZIF-8 ball milled at various times.....	S5
FIGURE S4. PXRD of crystalline CdIF-1 ball milled at various times.....	S6
FIGURE S5. PXRD of crystalline BIF-1-Li ball milled at various times.....	S6
FIGURE S6. PXRD of crystalline Na zeolite-X ball milled at various times.....	S7
FIGURE S7. PXRD of crystalline Na zeolite-Y ball milled at various times.....	S7
FIGURE S8. PXRD of crystalline ZSM-5 ball milled at various times .....	S8
FIGURE S9. PXRD of crystalline solvated ZIF-4 ball milled at various times.....	S8
FIGURE S10. PXRD of crystalline solvated ZIF-8 ball milled at various times.....	S9
FIGURE S11. PXRD of crystalline solvated Na zeolite-X ball milled at various times.....	S9
FIGURE S12. PXRD of crystalline solvated Na zeolite-Y ball milled at various times.....	S10
FIGURE S13. PXRD of crystalline solvated ZSM-5 ball milled at various times.....	S10

### **Thermogravimetric Curves of Solvated Samples**

FIGURE S14. Thermogravimetric curves of ZIF-8 loaded with Methanol.....	S11
FIGURE S15. Thermogravimetric curves of ZIF-4 loaded with Methanol.....	S11
FIGURE S16. Thermogravimetric curves of Na Zeolite-X loaded with Water.....	S12
FIGURE S17. Thermogravimetric curves of Na Zeolite-Y loaded with Water.....	S12
FIGURE S18. Thermogravimetric curves of ZSM-5 loaded with Water.....	S13

## Fourier Transform Infra Red Data

FIGURE S19. FT-IR for crystalline ZIF-4 and $a_m$ ZIF-4.....	S14
FIGURE S20. FT-IR for crystalline ZIF-zni and $a_m$ ZIF-zni.....	S14
FIGURE S21. FT-IR for crystalline ZIF-8 and $a_m$ ZIF-8.....	S15
FIGURE S22. FT-IR for crystalline CdIF-1 and $a_m$ ZIF-4.....	S15
FIGURE S23. FT-IR for crystalline BIF-1-Li and $a_m$ BIF-1-Li.....	S16
FIGURE S24. FT-IR for crystalline Na zeolite-X and $a_m$ Na zeolite-X.....	S16
FIGURE S25. FT-IR for crystalline Na zeolite-Y and $a_m$ Na zeolite-Y.....	S17
FIGURE S26. FT-IR for crystalline ZSM-5 and $a_m$ ZSM-5.....	S17

## Pycnometric Data

Table S1. Pycnometric Data for Crystalline and Amorphous Samples.....	S18
---	-----

## SEM Images

FIGURE S27. SEM images for ZIF-4 and $a_m$ ZIF-4.....	S19
FIGURE S28. SEM images for Na zeolite-Y and $a_m$ Na zeolite.....	S19

## Modified CdIF-1 Synthesis

FIGURE S29. Comparison of PXRD patterns for pure and impure CdIF-1.....	S20
---	-----

## $^1\text{H}$ NMR Data

FIGURE S30. $^1\text{H}$ NMR data crystalline CdIF-1 and $a_m$ CdIF-1-20.....	S21
---	-----

## $^1\text{H}$ - $^{15}\text{N}$ CP NMR Data

FIGURE S31. $^{15}\text{N}$ NMR data crystalline CdIF-1 and $a_m$ CdIF-1-20.....	S21
--	-----

## Powder X-ray Diffraction Data

All powder X-ray diffraction data was collected on a Bruker-AXS D8 diffractometer from a  $2\theta$  range 5-60° in Bragg-Brentano parafocusing geometry using a LynxEye position sensitive detector and radiation of (Cu  $K\alpha$ )1 ( $\lambda = 1.540598 \text{ \AA}$ ). The program X'pert HighScore Plus was used to analyse the resulting data.

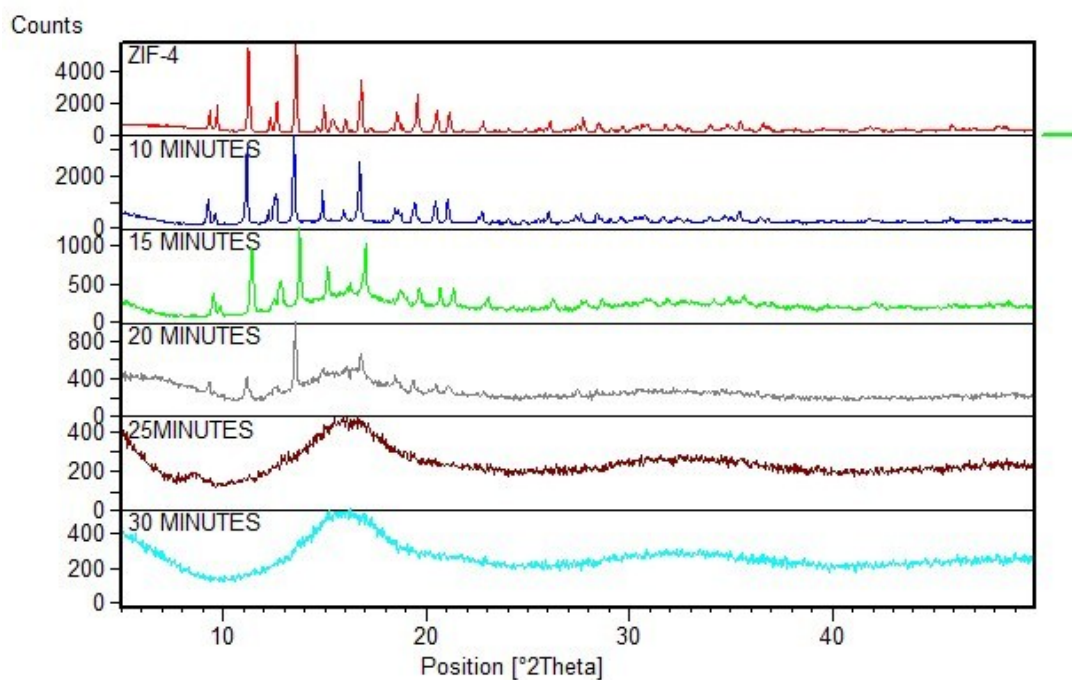


**Fig. S1** PXRD of crystalline ZIF-4 ball milled at various times.

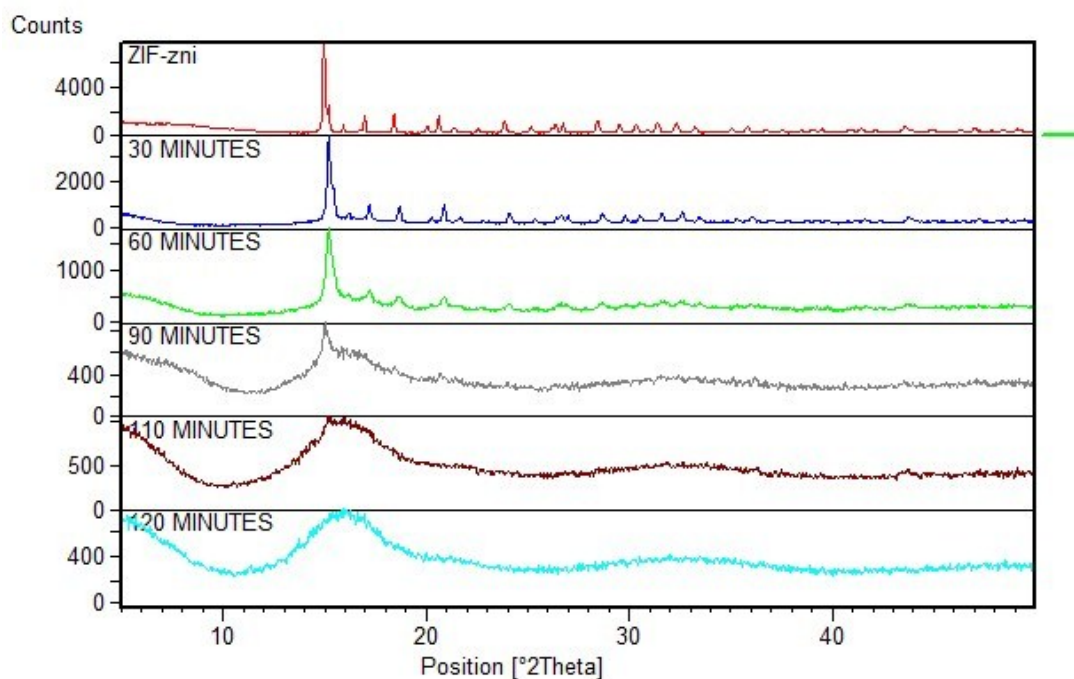


**Fig. S2** PXRD of crystalline ZIF-zni ball milled at various times.

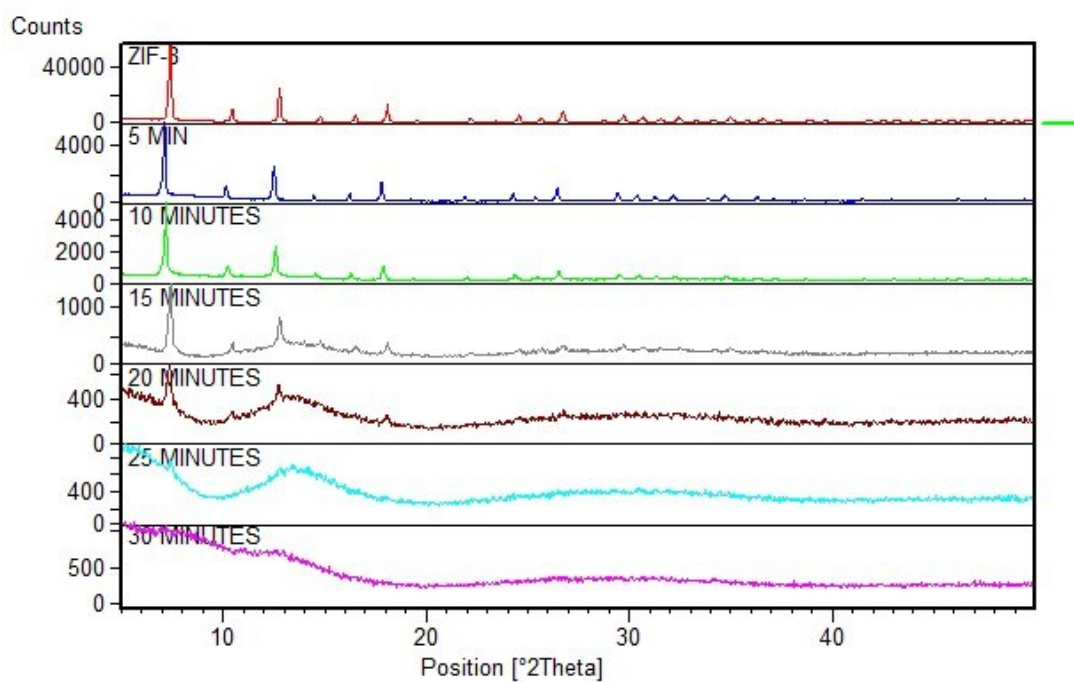


**Fig. S3** PXRD of crystalline ZIF-8 ball milled at various times.

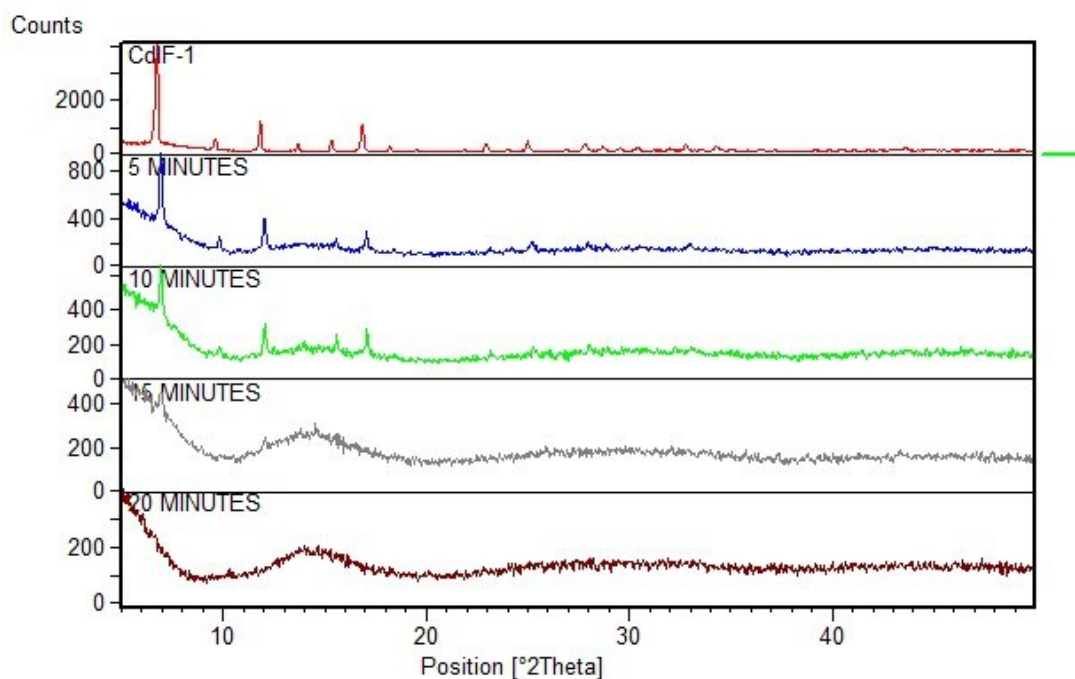


**Fig. S4** PXRD of crystalline CdIF-1 ball milled at various times.

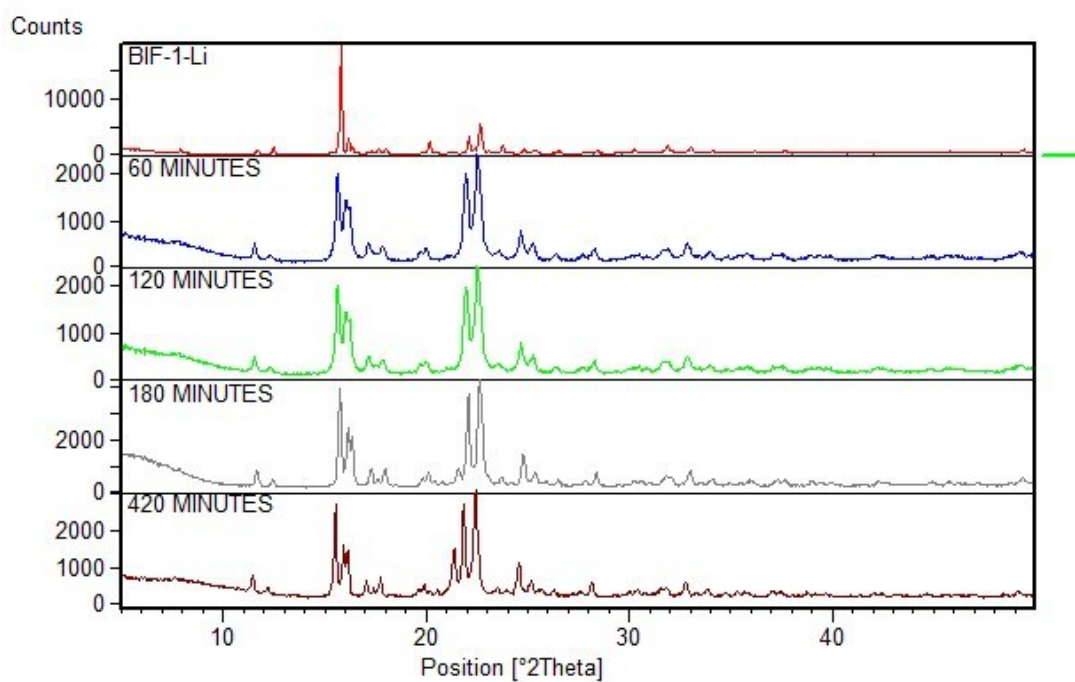


**Fig. S5** PXRD of crystalline BIF-1-Li ball milled at various times.

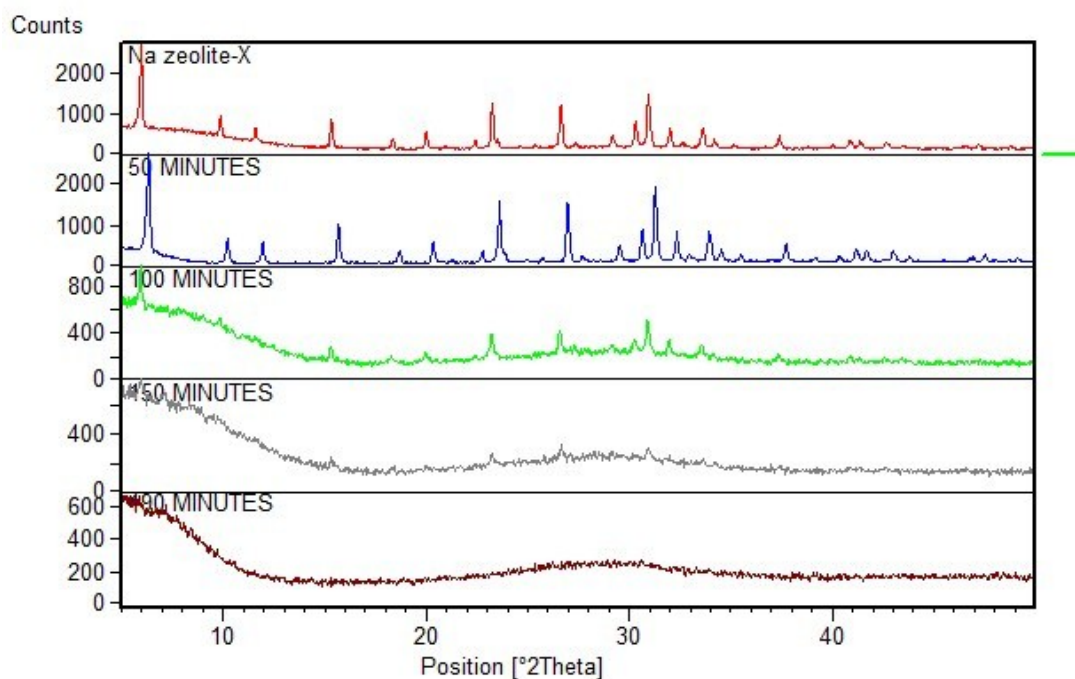


**Fig. S6** PXRD of crystalline Na zeolite-X ball milled at various times.

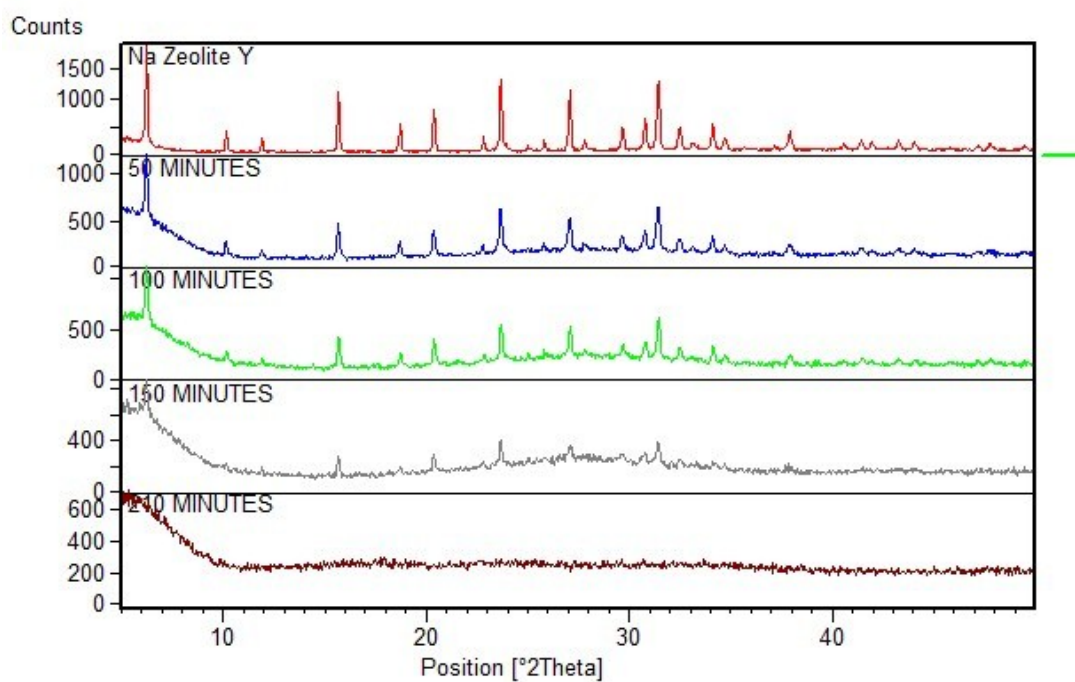


**Fig. S7** PXRD of crystalline Na zeolite-Y ball milled at various times.

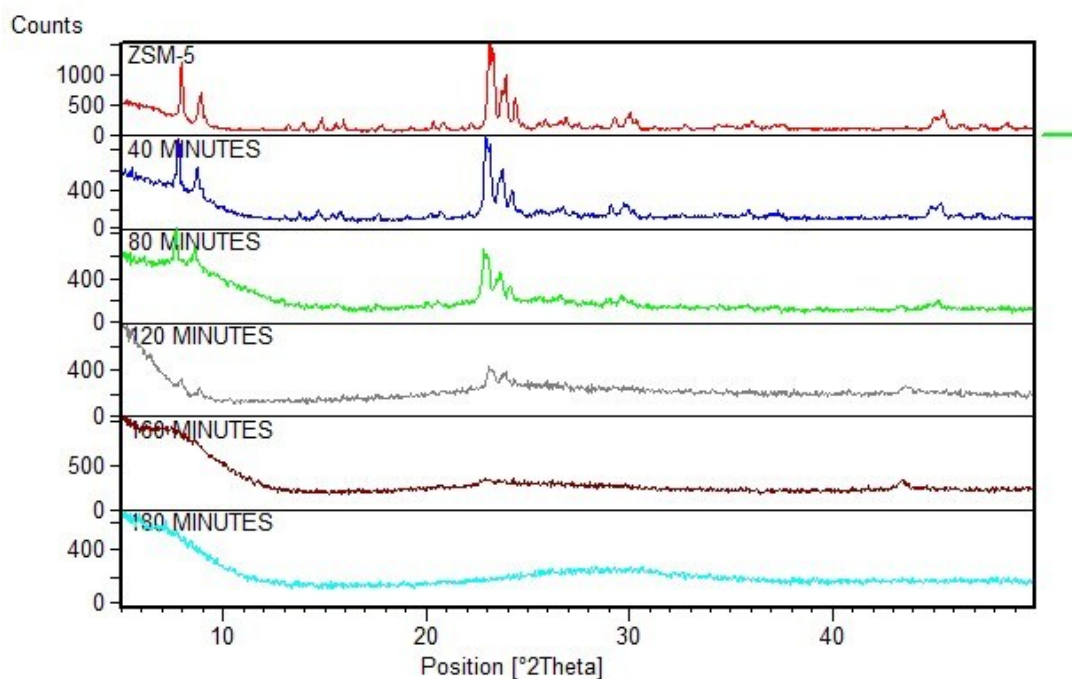


**Fig. S8** PXRD of crystalline ZSM-5 ball milled at various times.

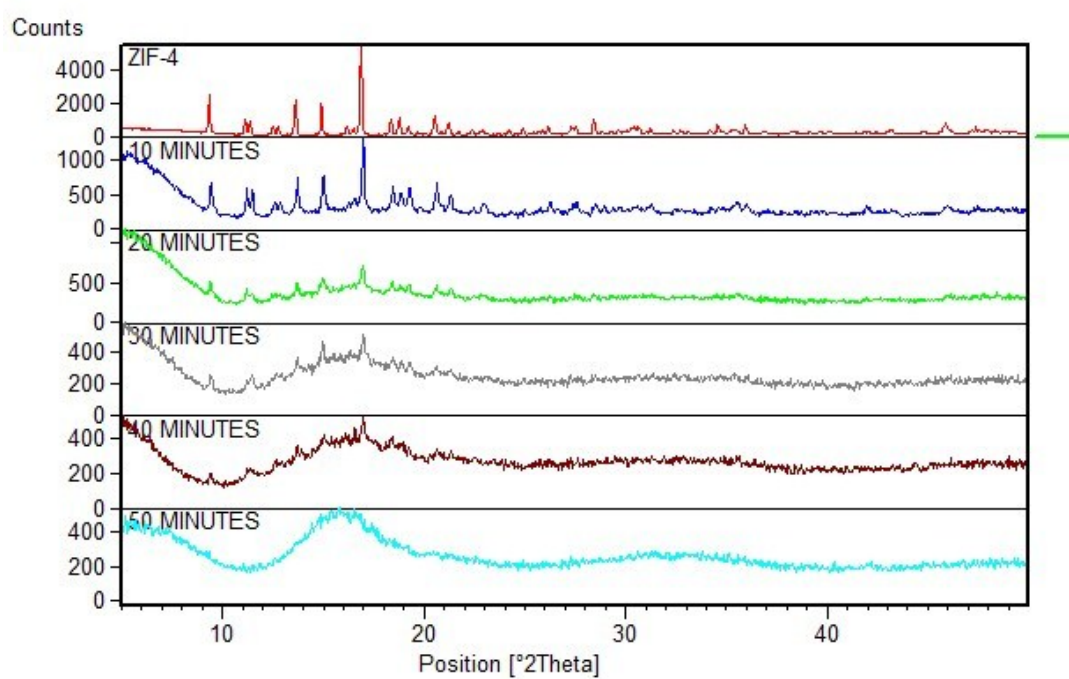


**Fig. S9** PXRD of crystalline solvated ZIF-4 ball milled at various times.



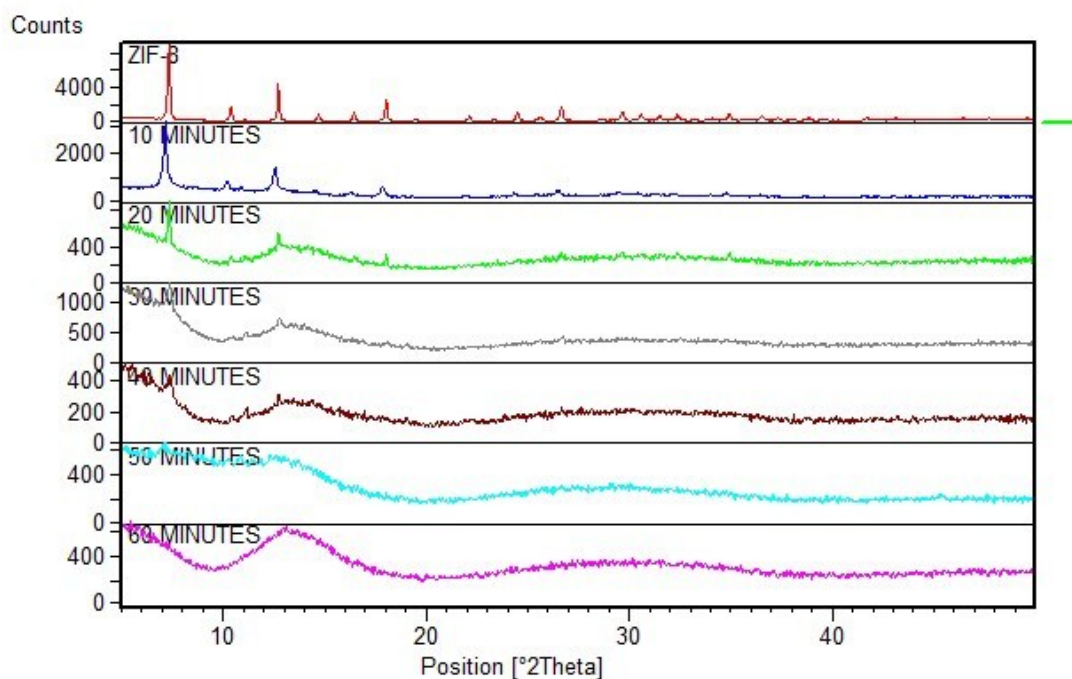


**Fig. S10** PXRD of crystalline solvated ZIF-8 ball milled at various times.

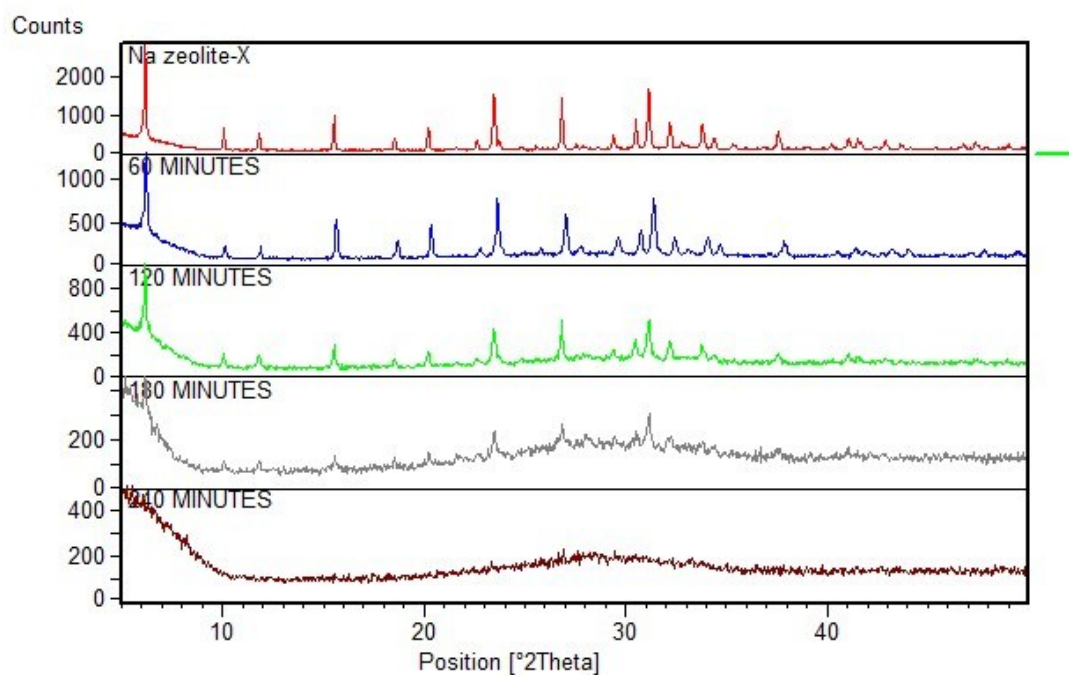


**Fig. S11** PXRD of crystalline solvated Na zeolite-X ball milled at various times.

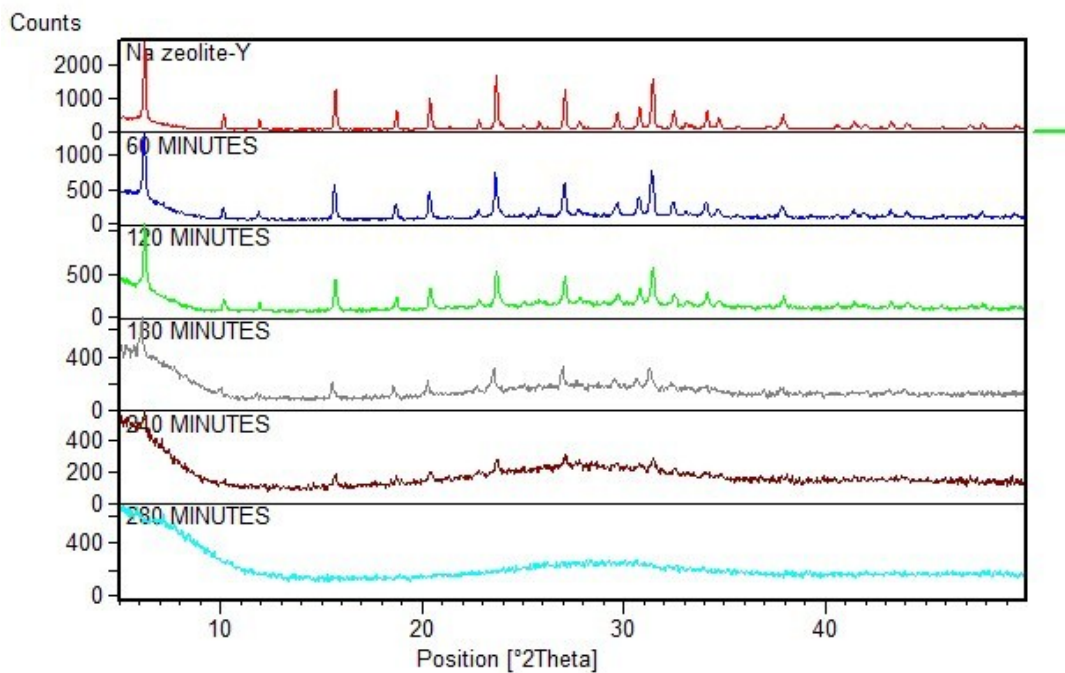


**Fig. S12** PXRD of crystalline solvated Na zeolite-Y ball milled at various times.

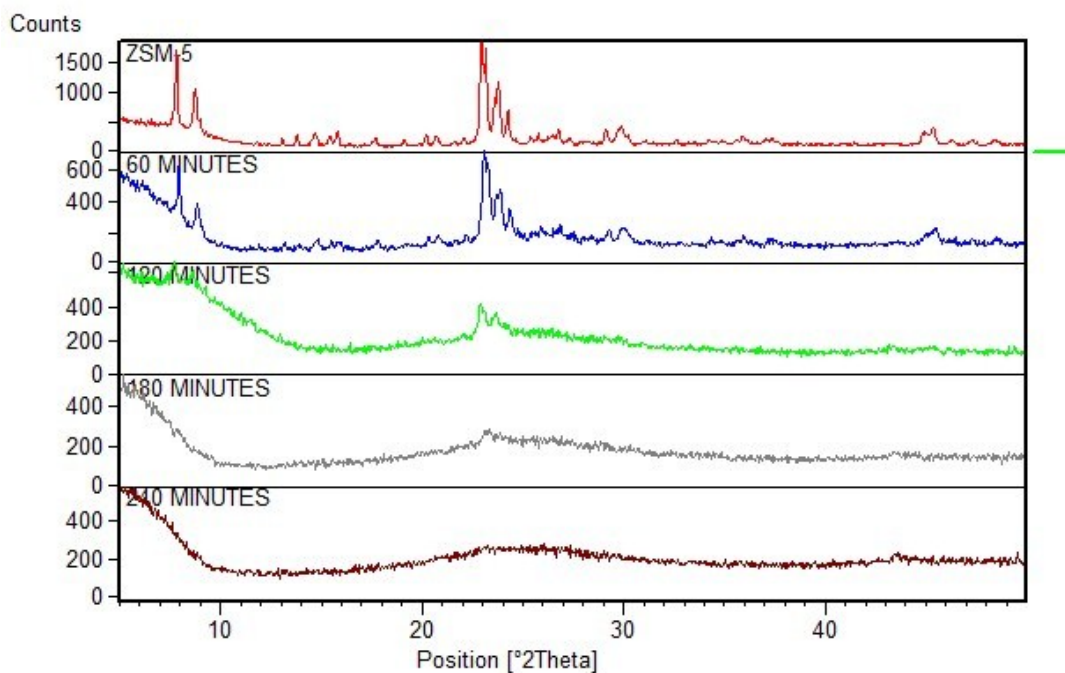


**Fig. S13** PXRD of crystalline solvated ZSM-5 ball milled at various times.

### Thermogravimetric Curves of Solvated Samples

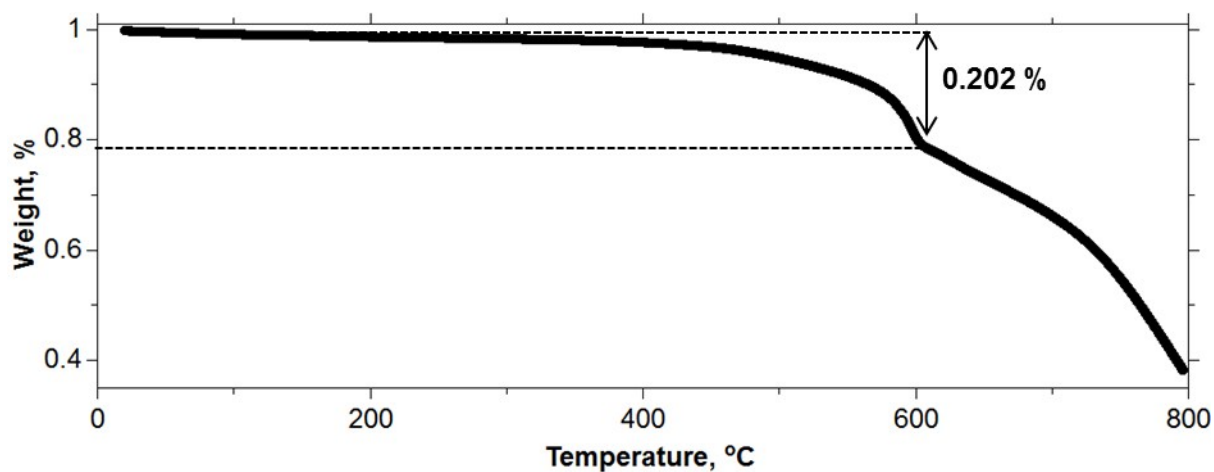


Fig. S14 TGA curve of ZIF-8 loaded with Methanol.

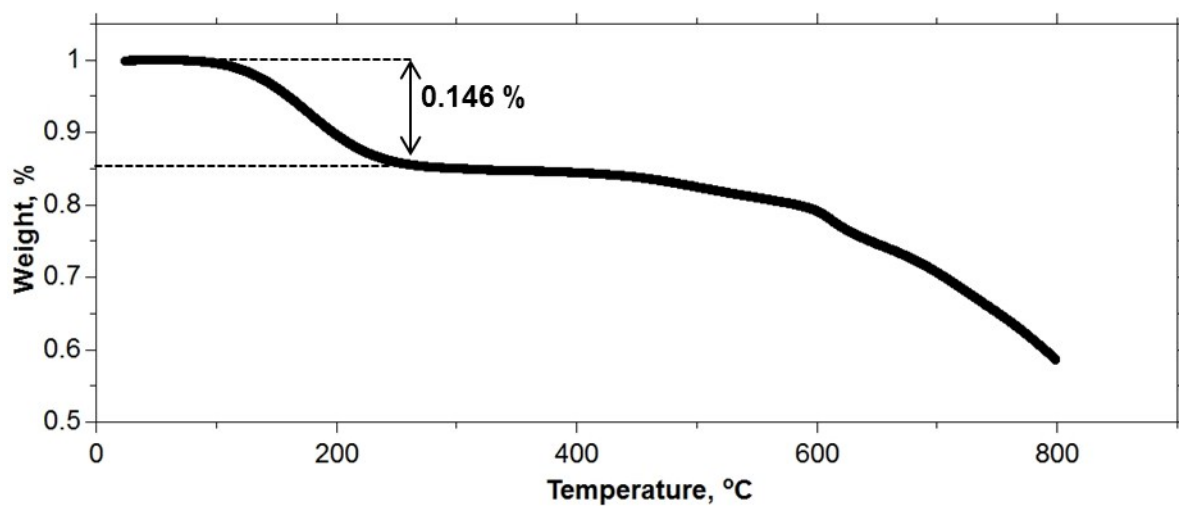
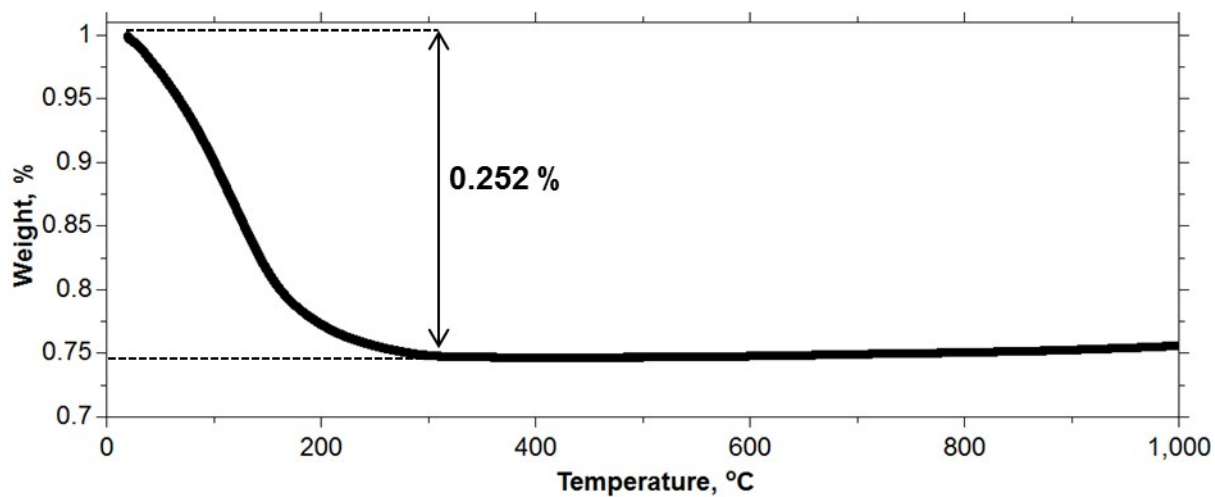
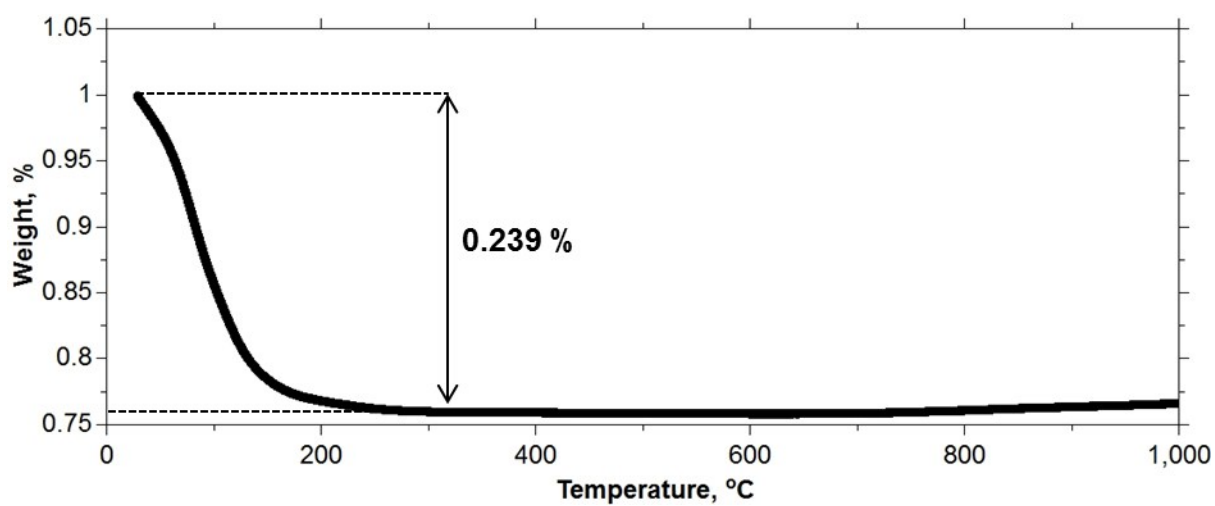


Fig. S15 TGA curve of ZIF-4 loaded with Methanol.



**Fig. S16** TGA curve of Na zeolite-X with water.



**Fig. S17** TGA curve of Na zeolite-Y with water.

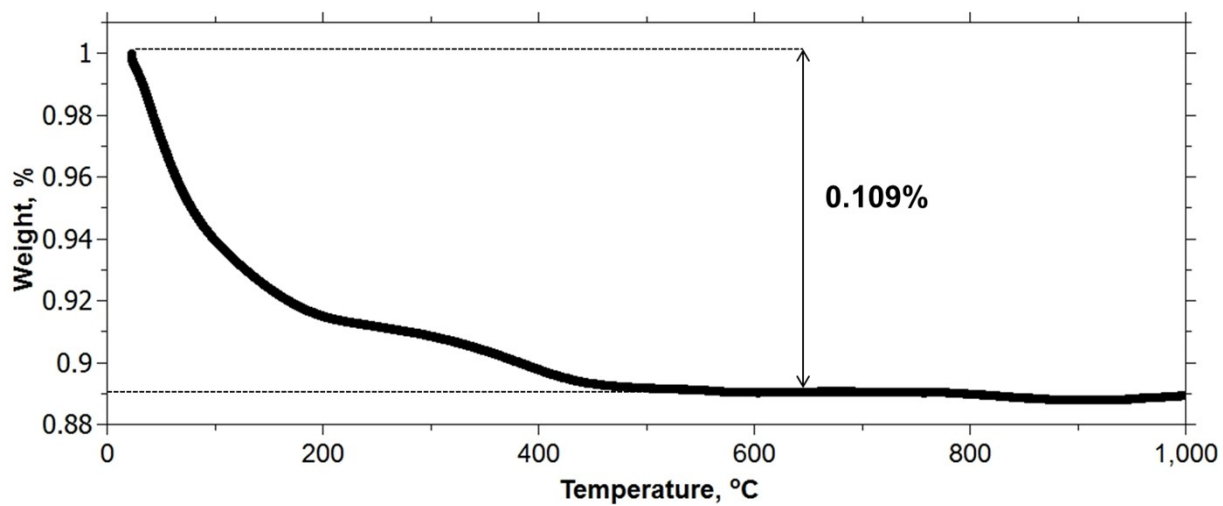


**Fig. S18** TGA curve of ZSM-5 with water.

## Fourier Transform Infra Red Data

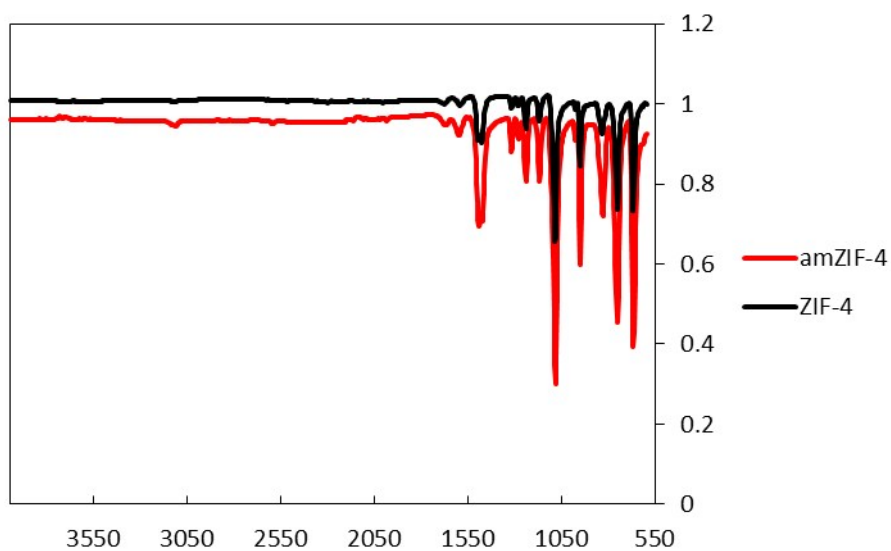


**Fig. S19** FT-IR for crystalline ZIF-4 and  $a_m$ ZIF-4.

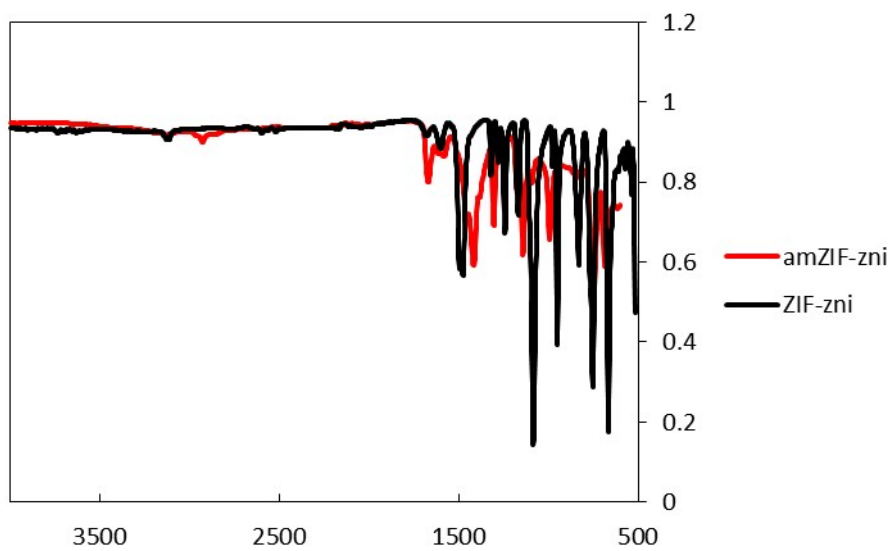


**Fig. S20** FT-IR for crystalline ZIF-zni and  $a_m$ ZIF-zni.

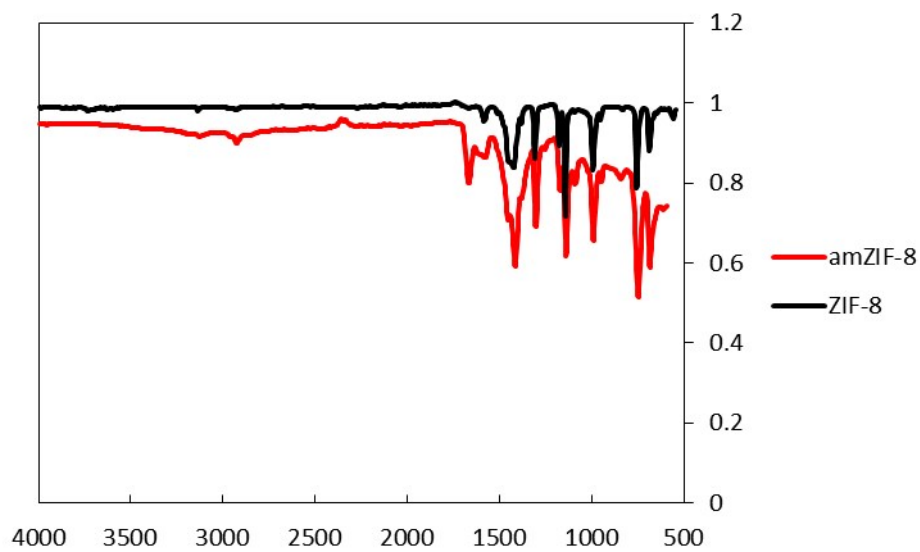


**Fig. S21** FT-IR for crystalline ZIF-8 and  $a_m$ ZIF-8.

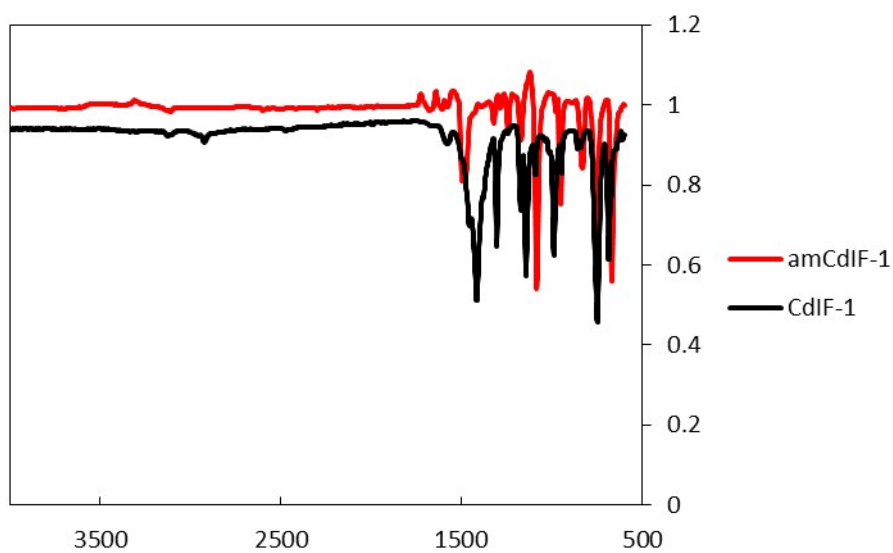


**Fig. S22** FT-IR for crystalline CdIF-1 and  $a_m$ CdIF-1-20. Note that there are differences in these spectra which may be related to the features seen in the NMR work.

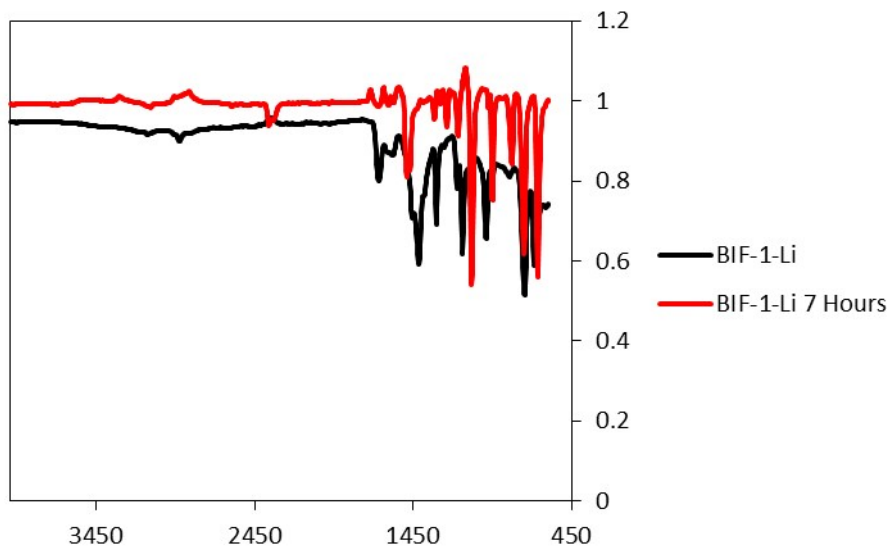


**Fig. S23** FT-IR for crystalline BIF-1-Li and  $a_m$ BIF-1-Li.

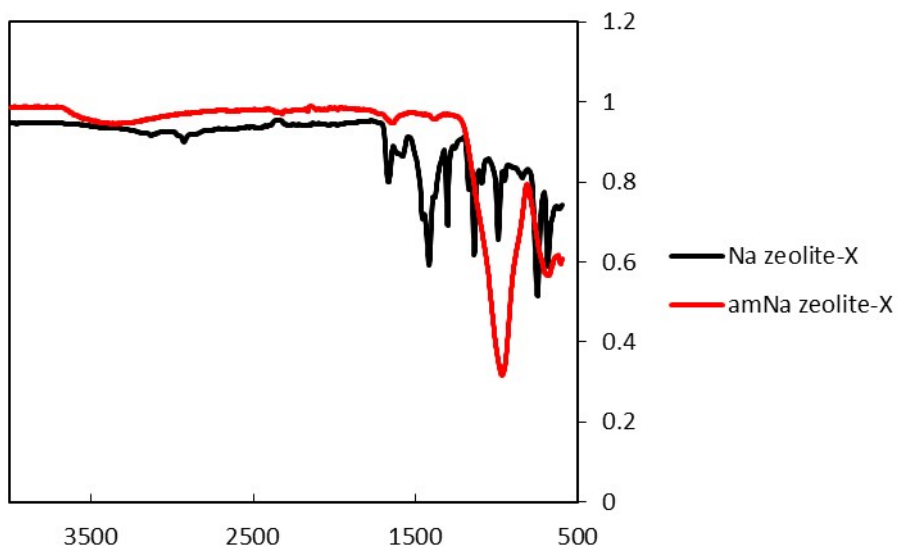


**Fig. S24** FT-IR for crystalline Na zeolite-X and  $a_m$ Na zeolite-X.



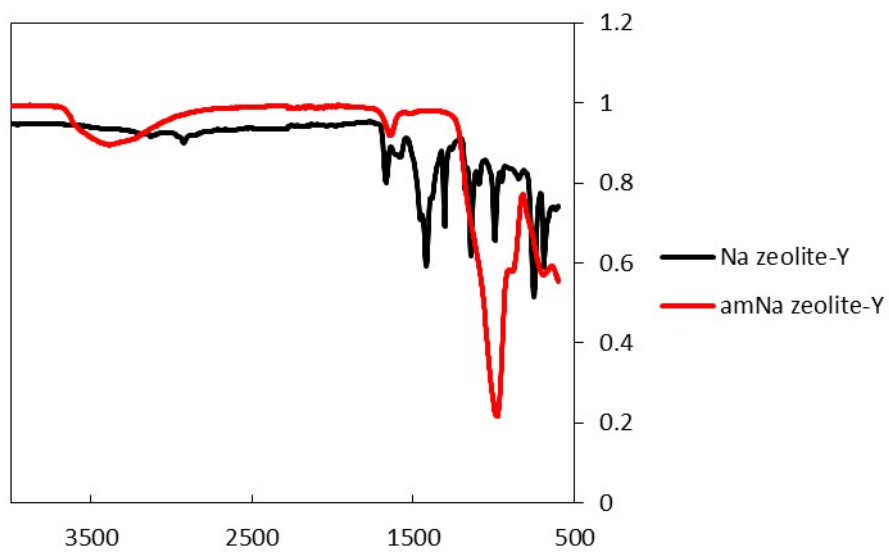


**Fig. S25** FT-IR for crystalline Na zeolite-Y and  $a_m$ Na zeolite-Y.

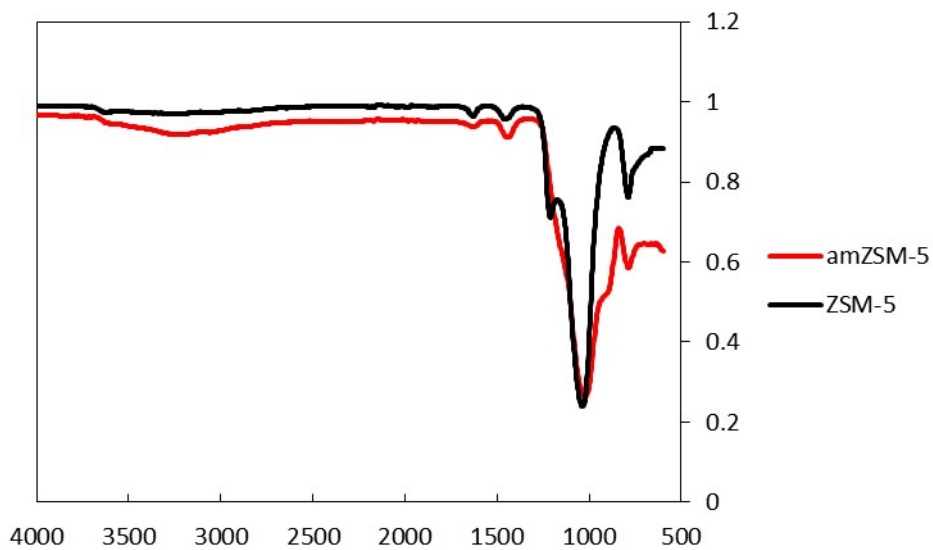


**Fig. S26** FT-IR for crystalline ZSM-5 and  $a_m$ ZSM-5.

## Pycnometric Data

Table S1 Pycnometric Data for Crystalline and Amorphous Samples

Framework	Pycnometric Density/g cm <sup>-3</sup>	Time taken to amorphize the sample/minutes
Na zeolite-Y	1.909(16)	210
<i>a<sub>m</sub></i> Na zeolite-Y	2.134(43)	-
Na zeolite-X	1.958(23)	190
<i>a<sub>m</sub></i> Na zeolite-X	2.443(41)	-
ZSM-5	2.234(33)	180
<i>a<sub>m</sub></i> ZSM-5	2.611(22)	-
ZIF-zni	1.612(19)	120
<i>a<sub>m</sub></i> ZIF-zni	1.624(12)	-
ZIF-8	1.451(01)	30
<i>a<sub>m</sub></i> ZIF-8	1.512(19)	-
ZIF-4	1.462(05)	30
<i>a<sub>m</sub></i> ZIF-4	1.57 <sup>4</sup> (12)	-
CdIF-1	0.923(22)	20
<i>a<sub>m</sub></i> CdIF-1	0.982(37)	-
BIF-1-Li	1.349(22)	-

## SEM Images

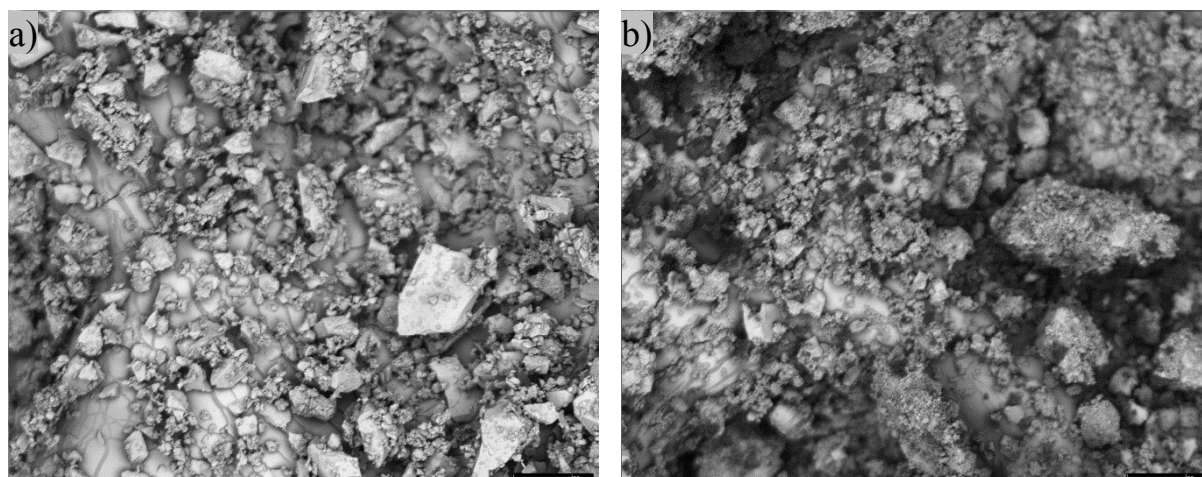


**Fig. S27** Back scattered SEM images at 400x magnification for a) ZIF-4 and b)  $a_m$ ZIF-4, scale bar = 30  $\mu\text{m}$ .

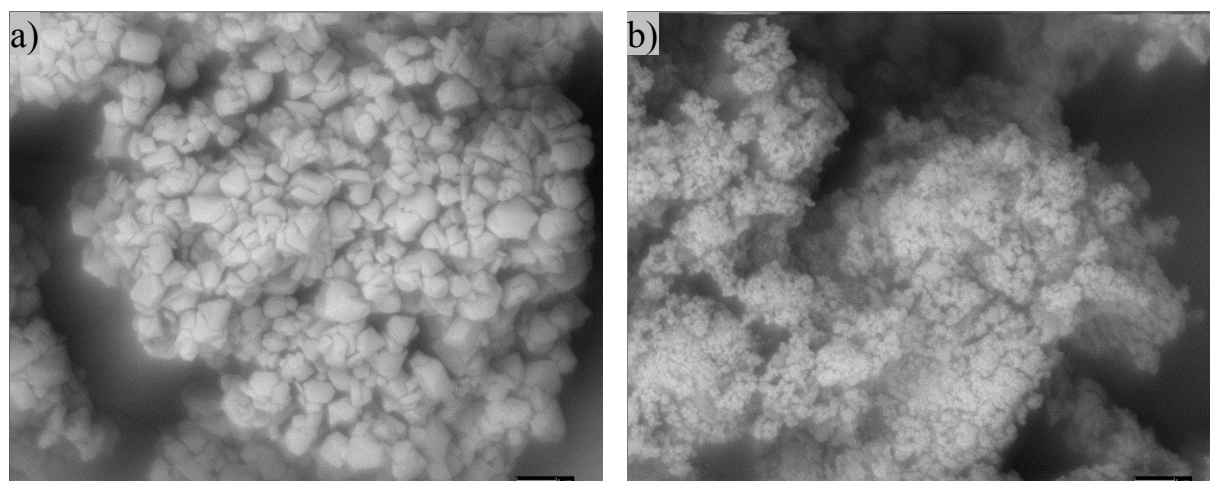


**Fig. S28** Back scattered SEM images at 8000x magnification for a) Na zeolite-Y and b)  $a_m$ Na zeolite-Y, scale bar = 1  $\mu\text{m}$ .

## Modified Synthesis of CdIF-1

The following synthesis was modified from a previously published procedure.<sup>1</sup> The original procedure resulted in an impurity (shown in Figure S29) at 14.5 and 16.5 °2 $\theta$ . By adjusting the temperature from 120 °C to 140 °C and the length of the reaction from 24 hours to 48 hours, only the pure CdIF-1 phase was formed. Unfortunately the CdIF-1 sample analysed using total-scattering techniques contained these impurities (Figure S18) which could explain the reduced data quality mentioned in the main paper, however the NMR samples were pure.

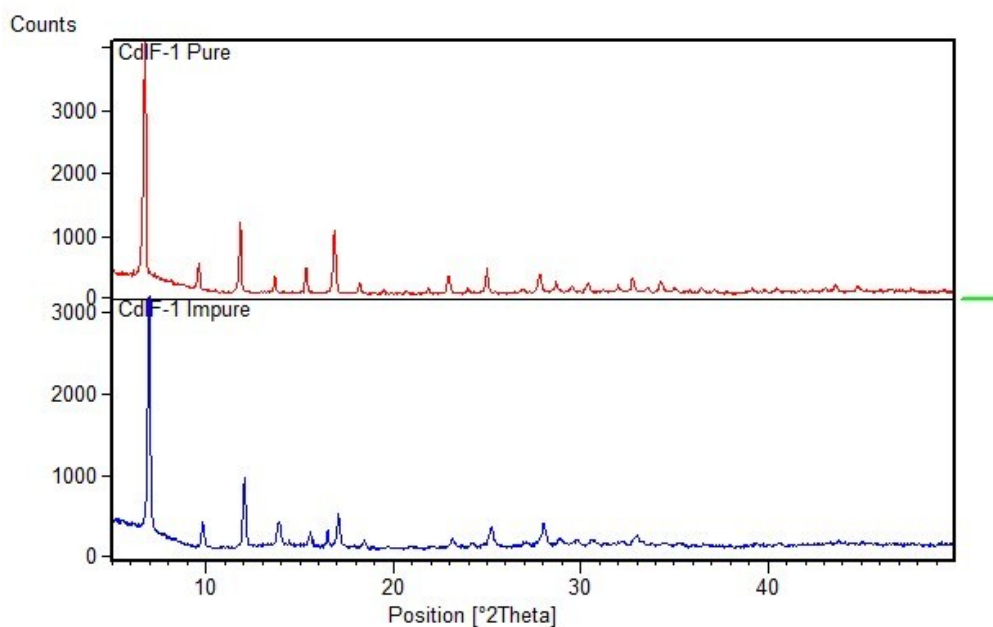


**Fig. S29** Comparison of PXRD patterns for pure and impure CdIF-1.

## $^1\text{H}$ NMR Data

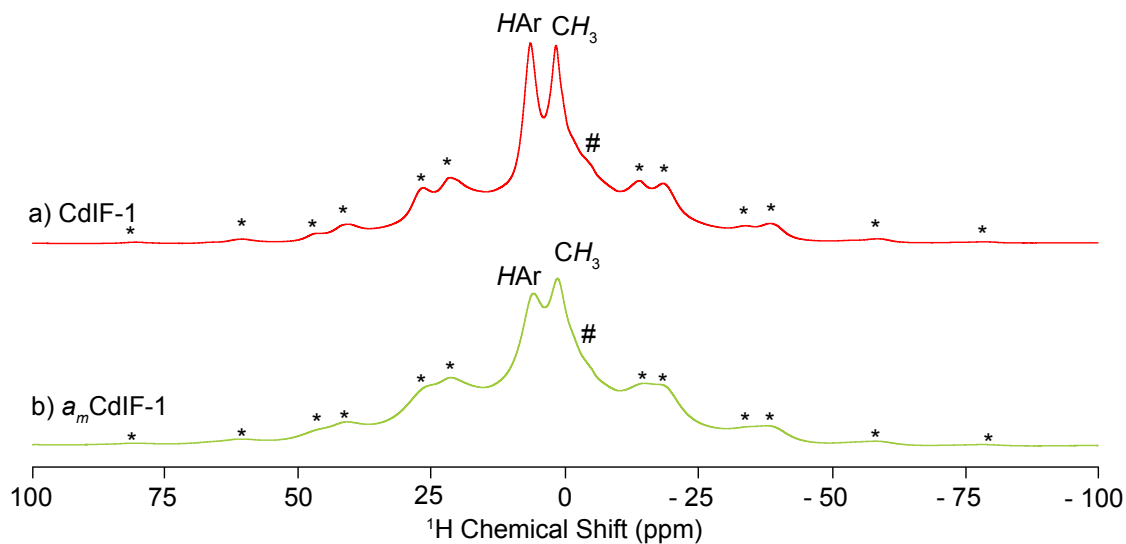


**Fig. S30**  $^1\text{H}$  MAS NMR spectra of a) CdIF-1 and b)  $a_m$ CdIF-1-20 obtained at 9.4 T Asterisks denote spinning sidebands.

## $^1\text{H}$ - $^{15}\text{N}$ CP NMR Data

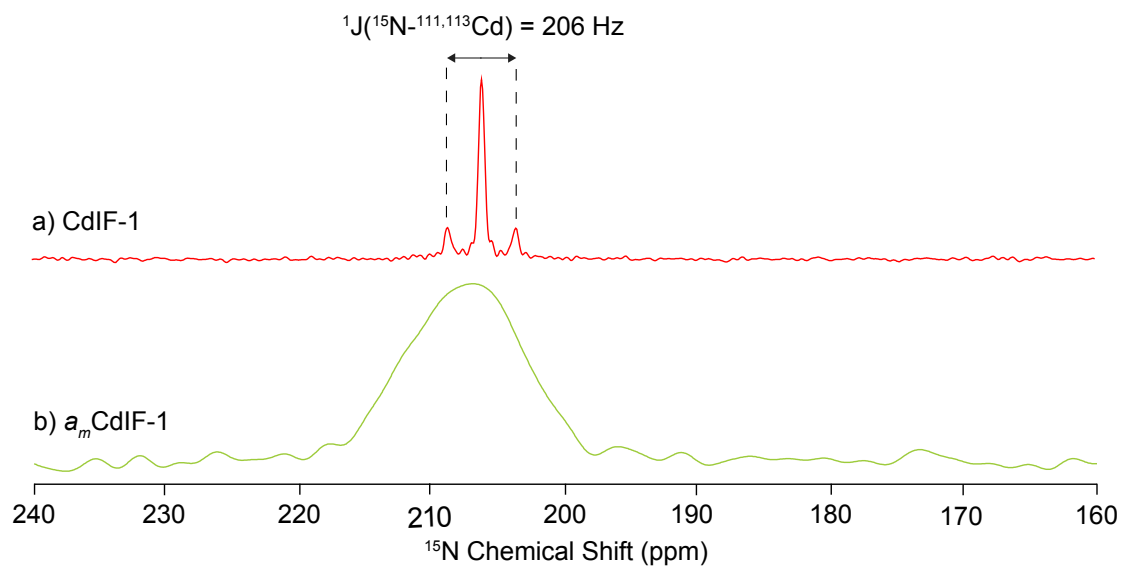


**Fig. S31**  $^{15}\text{N}$  CP MAS NMR spectra of a) CdIF-1 and b)  $a_m$ CdIF-1-20 recorded at 9.4 T. The coupling constant of the doublet arising from the indirect  $^1J(^{15}\text{N}-^{111,113}\text{Cd})$  spin spin coupling is given.

1. Y.-Q. Tian, S.-Y. Yao, D. Gu, K.-H. Cui, D.-W. Guo, G. Zhang, Z.-X. Chen and D.-Y. Zhao, *Chem. Eur. J.*, 2010, **16**, 1137-1141.